Crystal Structure, and the Infrared and Raman Spectra, of Tripotassium Methanetrisulphonate Hydrate, $K_3[CH(SO_3)_3]\cdot H_2O$

By **John R. Hall,* Robert A. Johnson,** and **Colin H. L. Kennard,** Department of Chemistry, University of Queensland, Brisbane, Australia 4067
Graham Smith, Department of Chemistry, Queensland Institute of Technology, Brisbane, Australia 4000

The crystal structure of the title compound has been determined using three-dimensional *X*-ray diffraction data, from 839 reflections; crystals are orthorhombic, space group $P2_12_12_1$, with unit-cell dimensions a = 9.405(1), b = 9.405(1), c = 12.321(1) Å, Z = 4. The structure has been solved using direct methods and refined by full-matrix least squares to R 0.045. The S–C–S angles (*ca.* 113°) indicate an expansion from tetrahedral stereochemistry and the S–C bond lengths (*ca.* 1.81 Å) are appreciably longer than those for $K_2[CH_2(SO_3)_2]$ (1.77 Å) and $Ca[CH_3SO_3]_2$ (1.75 Å). The i.r. (4 000—50 cm^{-1}) and Raman spectra of $K_3[CH(SO_3)_3]\cdot H_2O$ and $K_3[CD(SO_3)_3]\cdot D_2O$ at 77 K are reported and interpreted according to the crystal structure. To assist with the assignment, spectra of the anhydrous salt, $K_3[CH(SO_3)_3]$, and of aqueous solutions of the soluble lithium salts, have also been recorded. The SO_3 groups show their characteristic group frequencies: ν_{sym}(C–S) and ν_{asym}(C–S) are assigned to 762 and 820 cm^{-1}, respectively; $\delta_{sym}(CS_3)$ and $\delta_{asym}(CS_3)$ to 170 and *ca.* 210 cm^{-1}, respectively. I.r. spectra of samples containing the isotopically dilute HDO species confirm the presence of two types of hydrogen bond per water molecule.

As part of an investigation into the vibrational properties of the sulphonate derivatives of methane, ammonia, and hydroxylamine, we have recorded the i.r. and Raman spectra of polycrystalline tripotassium methanetrisulphonate hydrate, $K_3[CH(SO_3)_3]\cdot H_2O$ and $K_3[CD(SO_3)_3]\cdot D_2O$ at liquid nitrogen temperature. No vibrational data on the methanetrisulphonate ion have been published, although the spectrum of the methylsulphonate species, $[CH_3SO_3]^-$, has been reported.[1,2] In order to have an adequate prediction of the spectra, the crystal structure of $K_3[CH(SO_3)_3]\cdot H_2O$ was determined. To assist with the internal mode assignment for $[CH(SO_3)_3]^{3-}$ and $[CD(SO_3)_3]^{3-}$, the aqueous solution spectra, including qualitative Raman polarization data of the soluble lithium salts, have been obtained. The lattice-water assignment is assisted by comparison with the spectra of the anhydrous salt $K_3[CH(SO_3)_3]$, and of partially deuteriated $K_3[CH(SO_3)_3]\cdot H_2O$ samples.

EXPERIMENTAL

Preparations.—$K_3[CH(SO_3)_3]\cdot H_2O$ was prepared by the method described by Backer [3] (Found: C, 3.0; K, 30.1; H_2O, 4.7. Calc. for $CH_3K_3O_{10}S_3$: C, 3.1; K, 30.2; H_2O, 4.6%). Anhydrous $K_3[CH(SO_3)_3]$ was obtained by heating $K_3[CH(SO_3)_3]\cdot H_2O$ at 410 K at 1 atm for 12 h (Found: C, 3.4; K, 31.1. Calc. for $CHK_3O_9S_3$: C, 3.2; K, 31.7%). $Li_3[CH(SO_3)_3]\cdot 4H_2O$ was obtained by decomposing a suspension of the insoluble barium salt, $Ba_3[CH(SO_3)_3]_2\cdot 9H_2O$ [4,5] {obtained by addition of $BaCl_2\cdot 2H_2O$ solution to a boiling solution of $K_3[CH(SO_3)_3]\cdot H_2O$} with lithium sulphate. The resulting precipitate of $Ba[SO_4]$ was filtered off and the volume of the filtrate reduced until crystals of $Li_3[CH(SO_3)_3]\cdot 4H_2O$ [5] were deposited (Found: C, 3.7. Calc. for $CH_9Li_3O_{13}S_3$: C, 3.5%). $K_3[CD(SO_3)_3]\cdot D_2O$ was prepared by several recrystallizations of $K_3[CH(SO_3)_3]\cdot H_2O$ from the minimum quantity of boiling D_2O. Exchange of the methane hydrogen was almost complete. Exchange of the water hydrogen atoms was estimated from i.r. spectra to be *ca.* 85% (Found: C, 3.1; K, 30.0; D_2O, 5.1. Calc. for $CD_3K_3O_{10}S_3$: C, 3.1; K, 30.0; D_2O, 5.1%). $Li_3[CD(SO_3)_3]\cdot 4D_2O$ was prepared by the same procedure.

Partially deuteriated samples. These were prepared by the procedure previously described,[6] starting with 0.2 g of $K_3[CH(SO_3)_3]\cdot H_2O$ and recrystallizing from neutral H_2O–D_2O mixtures. The approximate concentrations of H_2O, HDO, and D_2O in the deuteriated samples were calculated by the method described by Seidl and Knop.[7]

Crystal Data.—$CH_3K_3O_{10}S_3$, M = 388.5, Orthorhombic, a = 9.405(1), b = 9.405(1), c = 12.321(1) Å, U = 1 090.0 Å^3, D_m = 2.40 g cm^{-3} (by flotation), Z = 4, D_c = 2.38 g cm^{-3}, $F(000)$ = 776, space group $P2_12_12_1$ (D_2^4, No. 19); Mo-K_α radiation, λ = 0.710 7 Å, μ(Mo-K_α) = 18.16 cm^{-1}.

Structure Determination.—Crystal and intensity data were obtained from a single crystal mounted about the b axis on a Hilger and Watts four-circle diffractometer. A total of 839 unique reflections with $F > 2.5\sigma(F)$ were considered observed out of 995, for an octant of the limiting sphere up to θ = 22°. Absorption corrections were not applied. The structure was solved using the TANG-non-centrosymmetric direct-methods approach incorporated in the *X*-ray crystallographic program set SHELX.[8] The oxygen atoms were located from the first weighted difference-Fourier. The methane hydrogen atom was found in a later difference map, and given the isotropic temperature factor of C(1) and included in the calculation, but its parameters were not refined. Full-matrix least-squares refinement, with anisotropic temperature factors for potassium and sulphur only, reduced R from an initial value of 0.42 to 0.045; unit weights were used. A final difference-Fourier revealed no peaks greater than 0.3 e Å^{-3}. The two hydrogens attached to the water oxygen could not be located from the difference map. Atomic parameters are listed in Table 1. Neutral element scattering factors were used,[9] and correction was applied for anomalous dispersion.[10] Observed and calculated structure amplitudes and atomic thermal parameters are listed in Supplementary Publication, No. SUP 22579 (7 pp.).†

I.r. Spectra.—I.r. spectra in the 4 000—400 cm^{-1} region were recorded on a Perkin-Elmer model 225 spectrophotometer and calibrated with polystyrene film. Solution samples were examined as thin films between KRS5 plates; solid samples were examined as Nujol mulls between CsI

† See Notices to Authors No. 7, *J.C.S. Dalton*, 1979, Index issue.

TABLE 1

Atomic co-ordinates ($\times 10^4$) and isotropic thermal parameters ($\times 10^3$) with estimated standard deviations in parentheses

Atom	x/a	y/b	z/c	U(Å²)
K(1)	7 504(3)	1 616(3)	6 691(2)	
K(2)	9 842(3)	5 028(4)	5 632(2)	
K(3)	2 895(4)	2 354(4)	7 134(3)	
S(1)	−842(3)	6 159(4)	10 013(3)	
S(2)	1 264(4)	3 776(4)	10 383(3)	
S(3)	−417(3)	3 884(4)	8 287(3)	
O(11)	−2 395(9)	6 200(10)	9 925(7)	21(2)
O(12)	−353(10)	6 474(10)	11 133(7)	21(2)
O(13)	−157(9)	7 042(10)	9 202(7)	15(2)
O(21)	2 253(10)	4 933(11)	10 257(8)	24(2)
O(22)	842(11)	3 537(12)	11 513(8)	31(3)
O(23)	1 669(10)	2 468(12)	9 853(9)	30(3)
O(31)	952(9)	4 311(10)	7 828(7)	17(2)
O(32)	−639(9)	2 346(10)	8 288(8)	17(2)
O(33)	−1 605(10)	4 648(10)	7 796(8)	22(4)
O(H)	40(13)	326(14)	1 707(10)	49(3)
C(1)	−402(13)	4 345(13)	9 711(9)	9(4)
H(1)	−1 154	3 986	9 789	9

plates, and as KBr discs. The cryostat used was of conventional design and fitted with KBr windows. Spectra in the region 400—50 cm^{-1} were run on a Beckman-RIIC IR-720 far-infrared spectrophotometer. Samples were examined as Nujol mulls between polythene plates mounted in a Beckman-RIIC VLT-2 variable-temperature unit. As a check on possible phase changes on cooling to liquid nitrogen temperature, the i.r. and Raman spectra of $K_3[CH(SO_3)_3]\cdot H_2O$ and $K_3[CH(SO_3)_3]$ were also recorded at ambient temperature. Apart from the general sharpening of bands and improved resolution at 77 K, there were no significant differences between the spectra.

Raman Spectra.—Raman spectra were recorded on a Cary model 82 laser spectrophotometer. An argon–krypton laser (Coherent Radiation, model 52 HD) was used to produce the exciting radiation (514.5 nm). Spectra were calibrated by reference to non-coherent discharge lines of the argon–krypton laser. Samples were held in a glass tube (4-mm diameter) mounted vertically to receive the laser beam through the optically flat base. The laser power at the sample was *ca.* 400 mW. The cryostat used was supplied by The Oxford Instrument Co. Ltd. (model CF100). The observed i.r. and Raman frequencies are estimated to be accurate to ± 2 cm^{-1} below 2 000 cm^{-1} and ± 4 cm^{-1} above 2 000 cm^{-1}.

RESULTS AND DISCUSSION

Crystal Structure.—The CS_3 skeleton of the $[CH(SO_3)_3]^{3-}$ ion (Figure 1) is distorted with all S–C–S angles greater than the tetrahedral angle [Table 2(*a*)]. All S–O bond lengths (mean 1.459 Å) and O–S–O angles (mean 112.7°) are similar to those found in the related compounds $K_2[CH_2(SO_3)_2]$ (1.461 Å, 113.3°),[11] $Ca[CH_3SO_3]_2$ (1.445 Å, 112.5°),[12] and $Cs[CH_3SO_3]$ (1.47 Å, 112°).[13] An unusual feature of the structure is that one C–S bond length [1.851(13) Å] is significantly greater than the other two [1.795(13) and 1.807(12) Å].

A comparison of the C–S bond length in $K_3[CH(SO_3)_3]\cdot H_2O$ (mean 1.813 Å) with those of $K_2[CH_2(SO_3)_2]$ (1.770 Å) and $Ca[CH_3SO_3]_2$ (1.754 Å) shows a tendency towards longer C–S bonds with the successive replacement of hydrogen atoms by SO_3 groups, presumably due to repulsion between the latter. This effect is also observed in the case of tris(methylsulphonyl)methane, $CH(CH_3SO_2)_3$ [14] and tris(ethylsulphonyl)methane, $CH(C_2H_5SO_2)_3$,[15] where the lengths of the C–S bonds which involve the methane carbon atoms (1.83 and 1.834 Å, respectively) are considerably greater than those which involve the methyl (1.73 Å) and ethyl (1.785 Å) carbon atoms.

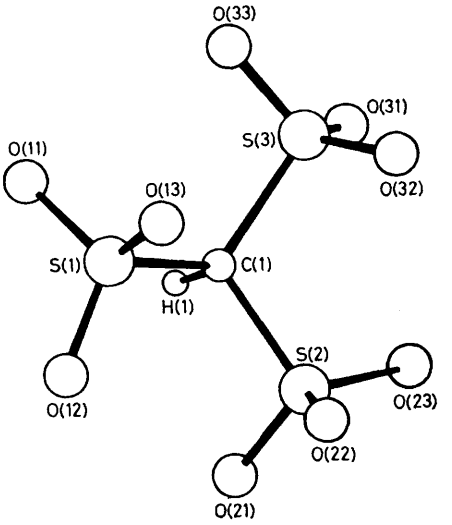

FIGURE 1 Atomic numbering system and structure of an individual $[CH(SO_3)_3]^{3-}$ ion viewed perpendicular to the plane of S(3), C(1), and S(2)

The C–S bond length in $[Cu(CH_3SO_3)_2(H_2O)_4]$ (1.754 Å) [16] is consistent with this scheme but in $Cs[CH_3SO_3]$ (1.80 Å) it is slightly larger for the uncorrected distance. The

TABLE 2

(*a*) Interatomic distances (Å) and angles (°) for $[CH(SO_3)_3]^{3-}$ with estimated standard deviations given in parentheses

(*i*) Distances

C(1)–S(1)	1.795(13)	S(2)–O(21)	1.440(11)
C(1)–S(2)	1.851(13)	S(2)–O(22)	1.465(11)
C(1)–S(3)	1.807(12)	S(2)–O(23)	1.444(12)
S(1)–O(11)	1.465(9)	S(3)–O(31)	1.462(9)
S(1)–O(12)	1.484(9)	S(3)–O(32)	1.461(10)
S(1)–O(13)	1.450(10)	S(3)–O(33)	1.460(10)

(*ii*) Angles

S(1)–C(1)–S(2)	112.2(5)	C(1)–S(3)–O(33)	106.9(2)
S(1)–C(1)–S(3)	115.3(5)	O(11)–S(1)–O(12)	111.9(2)
S(2)–C(1)–S(3)	111.8(5)	O(11)–S(1)–O(13)	112.1(3)
C(1)–S(1)–O(11)	103.9(2)	O(12)–S(1)–O(13)	112.9(3)
C(1)–S(1)–O(12)	108.1(3)	O(21)–S(2)–O(22)	113.2(3)
C(1)–S(1)–O(13)	107.4(3)	O(21)–S(2)–O(23)	115.1(3)
C(1)–S(2)–O(21)	106.3(2)	O(22)–S(2)–O(23)	111.7(3)
C(1)–S(2)–O(22)	103.9(2)	O(31)–S(3)–O(32)	113.4(2)
C(1)–S(2)–O(23)	105.5(3)	O(31)–S(3)–O(33)	112.2(3)
C(1)–S(3)–O(31)	107.6(2)	O(32)–S(3)–O(33)	112.2(3)
C(1)–S(3)–O(32)	103.8(2)		

(*b*) Interatomic K–O distances (Å) less than 3.4 Å. Means include only those distances less than 3.1 Å.

	O(11)	O(12)	O(13)	O(21)	O(22)	O(23)
K(1)	2.994	2.791	2.756	2.884	2.713	
K(2)	2.718		2.831	2.771		2.765
K(3)	2.799	2.843	3.070		3.341	
	O(31)	O(32)	O(33)	O(H)	Mean	
K(1)	2.676	2.719		3.010	2.818	
K(2)	2.977	2.662	3.015	2.898	2.830	
K(3)	2.731		2.821		2.853	
				Grand Mean	2.834	

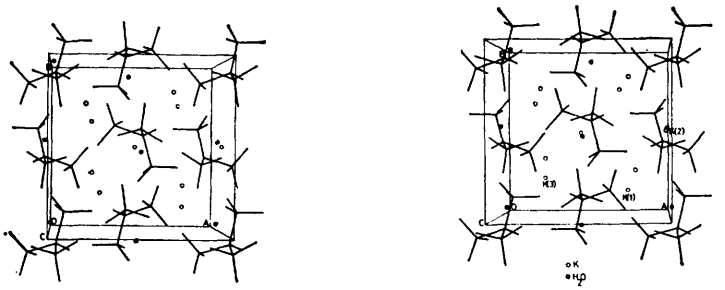

FIGURE 2 Stereoscopic view of the packing of $K_2[CH(SO_3)_3]\cdot H_2O$ in the cell viewed down the c axis

corrected distance is 1.85 Å. The packing of molecules in the unit cell is illustrated in Figure 2. The potassium ions are surrounded by five to eight oxygen atoms from the sulphonate groups or water molecule [Table 2(*b*)] at distances ranging from 2.662 to 3.070 Å. Intraionic and other short O–O contacts less than 3.2 Å are O(11)–O(33), 3.092; O(12)–O(21), 3.045; O(12)–O(22), 3.019; O(12)–O(H), 2.887; O(13)–O(33), 3.150; O(22)–O(H), 2.886; and O(23)–O(32), 2.906 Å.

Vibrational Investigation.—For an isolated $[CH(SO_3)_3]^{3-}$ ion of C_{3v} symmetry, the 36 normal modes of vibration are distributed among the symmetry species as follows, $8A_1 + 4A_2 + 12E$. The A_1 and E modes are i.r. and Raman active, whereas the A_2 modes are i.r. and Raman inactive. Approximate descriptions of these modes in terms of internal co-ordinate contributions are given in Table 3. Considerable mixing of these motions is expected in the actual normal modes. In the crystal, all atoms of the $K_3[CH(SO_3)_3]\cdot H_2O$ unit occupy general positions and hence factor-group analysis yields the vibrational representation shown in Table 4 (acoustic modes omitted). The A modes are Raman active only, whereas the B_1, B_2, and B_3 modes are i.r. and Raman active. The correlation between point, site, and unit-cell symmetry species is given in Table 5. The i.r. and Raman spectra of $K_3[CH(SO_3)_3]\cdot H_2O$ at 77 K are shown in Figure 3. The observed frequencies {including those for $K_3[CD(SO_3)_3]\cdot D_2O$ and aqueous (H_2O or D_2O) solutions of $Li_3[CH(SO_3)_3]\cdot 4H_2O$ and $Li_3[CD(SO_3)_3]\cdot 4D_2O$} and their assignments are given in Table 6.

The assignment of the polarized Raman bands at 2 952 and 2 210 cm^{-1} to the C–H and C–D stretches (A_1), respectively, is straightforward. Correlation field splitting of both modes is observed in the solid-state Raman

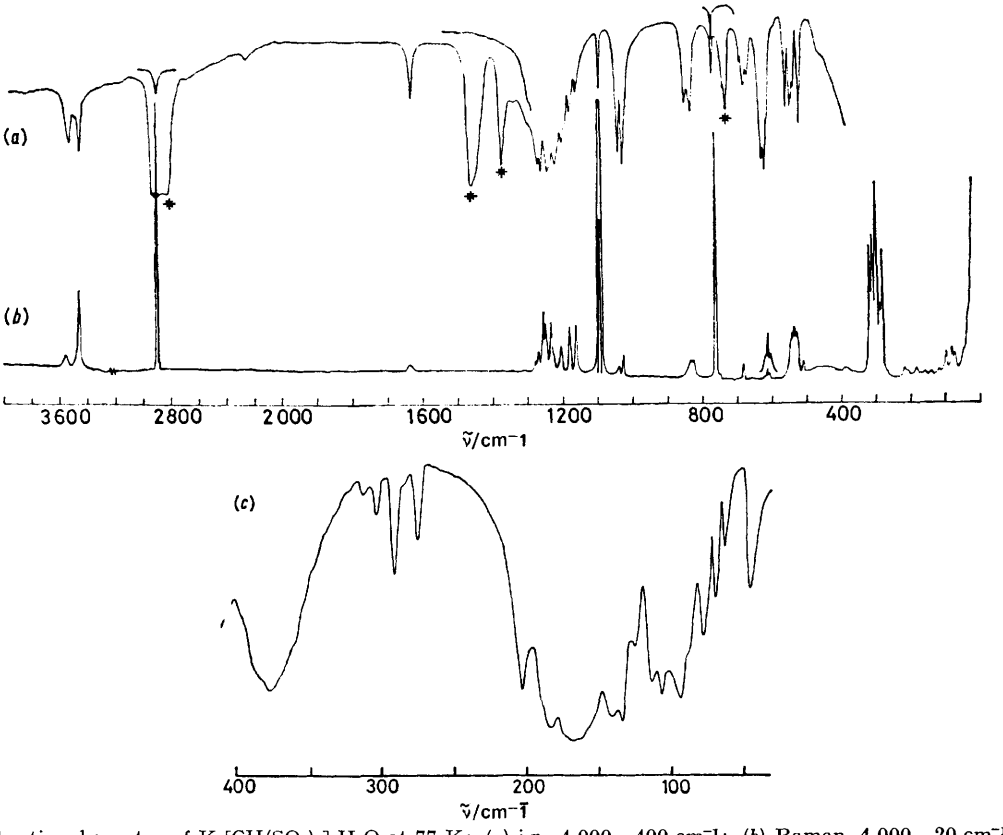

FIGURE 3 Vibrational spectra of $K_3[CH(SO_3)_3]\cdot H_2O$ at 77 K; (*a*) i.r., 4 000—400 cm^{-1}; (*b*) Raman, 4 000—20 cm^{-1}; and (*c*) i.r., 400—50 cm^{-1} (peaks marked * are due to Nujol)

TABLE 3

Approximate internal co-ordinate contributions to the vibrational modes of $[CH(SO_3)_3]^{3-}$ (C_{3v})

C–H stretch	A_1
HCS deformations	E
C–S stretches	$A_1 + E$
CS_3 deformations	$A_1 + E$
S–O stretches	$2A_1 + A_2 + 3E$
SO_3 deformations	$2A_1 + A_2 + 3E$
SO_3 rocks	$A_1 + A_2 + 2E$
SO_3 torsions	$A_2 + E$

TABLE 4

Vibrational representation for $K_3[CH(SO_3)_3]\cdot H_2O$

Γ(internal $[CH(SO_3)_3]^{3-}$ modes)	$36\ (A + B_1 + B_2 + B_3)$
Γ(internal H_2O modes)	$3(A + B_1 + B_2 + B_3)$
Γ(rotatory modes)	$6(A + B_1 + B_2 + B_3)$
Γ(translatory modes)	$15A + 14B_1 + 14B_2 + 14B_3$

TABLE 5

Correlation scheme for $K_3[CH(SO_3)_3]\cdot H_2O$

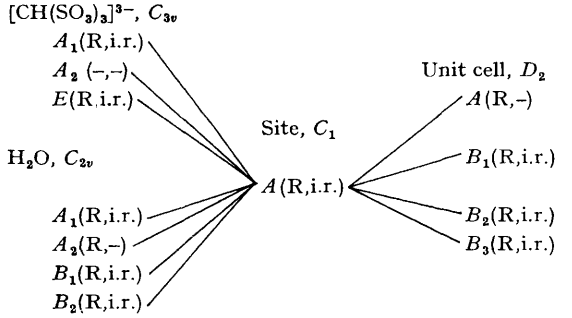

spectra where, in both cases, a weak shoulder appears on the low-frequency side of a relatively intense component.

The assignment of the weak, depolarized Raman band at 1 155 cm^{-1} to antisymmetric (E) modes which are mainly HCS bending in character is made on the basis of its observed isotopic frequency ratio, ν_H/ν_D (1.22), and by comparison with the frequency of the CH_3 rocking modes of $[CH_3SO_3]^-$ (967 cm^{-1}).[2] These modes appear as doublets in both the i.r. and Raman spectra of the solid, presumably through loss of degeneracy under the influence of the static crystal field. No other features ascribable to the anion above 820 cm^{-1}, apart from the C–H stretching bands, show major isotopic frequency shifts.

In the Raman solution spectrum, five other bands are observed in the region normally ascribed to S–O stretching (1 000—1 300 cm^{-1}), in accordance with predictions. The strong, polarized line at 1 092 cm^{-1} is attributed to symmetric S–O stretching (*cf.*[2] 1 049 cm^{-1} in $[CH_3SO_3]^-$). The weak band of uncertain polarization at 1 030 cm^{-1} is assigned to antisymmetric (E) S–O stretches since it appears as a doublet in both the i.r. and Raman spectra of the solid. The other band of uncertain polarization (1 240 cm^{-1}) is assigned to an A_1 mode since the correct number of depolarized bands corresponding to the remaining antisymmetric modes ($2E$) is observed (at 1 202 and 1 258 cm^{-1}). Collectively, the modes in the 1 200—1 300 cm^{-1} region ($A_1 + 2E$) are split into at least ten components in the solid-state spectrum. No assignment is made for the S–O stretch of A_2 species which obtains activity only through solid-state effects.

The weak, depolarized band at 820 cm^{-1} and the polarized band at 762 cm^{-1} in the Raman spectrum of $[CH(SO_3)_3]^{3-}$ are assigned to the antisymmetric (E) and symmetric (A_1) C–S stretching modes respectively by analogy with the C–S stretch of $[CH_3SO_3]^-$ (784 cm^{-1}).[2] In the solid, the degeneracy of the antisymmetric modes is lifted by the lower site symmetry to give doublets * in both the i.r. and Raman, with one component of the i.r. doublet being further split by the correlation field. Correlation coupling between symmetric C–S stretching modes is apparent in the Raman spectrum where two features are observed. These assignments are supported by isotropic (deuterium) frequency shifts, *ca.* 90 (E) and 12 cm^{-1} (A_1), respectively. In the Raman solution spectrum of $[CD(SO_3)_3]^{3-}$, the band ascribable to the E modes is masked by the more intense band at 750 cm^{-1}. However, unmasked bands ascribable to the former are apparent in the i.r. (738 cm^{-1}) and Raman spectra (739 cm^{-1}) of the solid.

The SO_3 and CS_3 bending and the SO_3 rocking vibrations are crowded together in the region below 700 cm^{-1} and hence considerable vibrational coupling between these vibrations is expected. However, it is a reasonable assumption that modes having predominantly SO_3 bending character will generally occur at higher frequencies than those which are predominantly SO_3 rocking. This is consistent with the assignments [2] made for the SO_3 bending (528 and 557 cm^{-1}) and rocking modes (347 cm^{-1}) of $[CH_3SO_3]^-$. Also, modes having appreciable contributions from bending vibrations of the CS_3 skeleton are expected to occur below those associated mainly with the SO_3 groups, as in the case of their respective stretching frequencies.

On this basis, the three polarized bands observed in this region are assigned to the symmetric (A_1), SO_3 bending (680 and 522 cm^{-1}), and rocking modes (290 cm^{-1}), and the three depolarized bands to the antisymmetric (E) SO_3 bending modes. The latter show both site and factor-group splitting in the solid-state spectrum. Doublets in the 310—320 and 280—290 cm^{-1} regions respectively of the solid-state spectrum are assigned to the antisymmetric (E) rocking modes. The weak shoulder at 583 cm^{-1} in the i.r. spectrum of the solid may be due to factor-group splitting of the E modes which give rise to the group of bands in the 605—620 cm^{-1} region. However, we prefer to assign this feature to the A_2 SO_3 bending mode because of its relatively large displacement (22 cm^{-1}) from the latter. Also, the very weak band at 465 cm^{-1} in the ambient-temperature i.r. spectrum of $K_3[CH(SO_3)_3]\cdot H_2O$ is assigned to the A_2 SO_3 rocking mode. Masking by the strong absorption of the KBr windows of the cryostat prevented the detection of this band in the low-temper-

* That these doublets are due to site effects and not to correlation field splitting is indicated by the presence of residual doublet bands of the isotopically dilute $[CH(SO_3)_3]^{3-}$ species in the i.r. spectrum of $K_3[CD(SO_3)_3]\cdot D_2O$.

TABLE 6

Observed frequencies and assignments for $[CH(SO_3)_3]^{3-}$ and $[CD(SO_3)_3]^{3-}$ ions, $K_3[CH(SO_3)_3]\cdot H_2O$ and $K_3[CD(SO_3)_3]\cdot D_2O$

0.1mol dm^{-3} $[CH(SO_3)_3]^{3-}$ Raman (and i.r.)	0.1mol dm^{-3} $[CD(SO_3)_3]^{3-}$ Raman (and i.r.)	$K_3[CH(SO_3)_3]\cdot H_2O$ (77 K) Raman	$K_3[CH(SO_3)_3]\cdot H_2O$ (77 K) I.r.	$K_3[CD(SO_3)_3]\cdot D_2O$ (77 K) Raman	$K_3[CD(SO_3)_3]\cdot D_2O$ (77 K) I.r.	Assignment
		47vw	52vw	46vw	49vw	lattice modes
		72w	69vw	72w	70vw	
			76vw		76vw	
		81w	84vw	80w	83vw	
			93sh		93sh	
		98w	100w	100w	97w	
			112w		109vw	
		117vw	119w	118vw	119w	
			132w		131w	
		141vw	140w	140vw	140w	
			148w			
		160vw		160vw		
		185w	189w	187vw,br	186w	
			170w,br		165w,br	$\delta(CS_3)$ (A_1)
		213sh	210w		207w	$\delta(CS_3)$ (E)
		219w		219w		
		283m	282vw	281m	277w	$\rho(SO_3)$ (E)
		290w	292sh	298sh	287sh	
290m,p	292m,p	301s	289vw	302s	292w	$\rho(SO_3)$ (A_1)
		311m	310vw	311s	300sh	$\rho(SO_3)$ (E)
		320m	319vw	318s	308vw	
					ca. 325vw,br	HDO rock (A')
		390w,br	380w,br		380vw,br	H_2O rock (B_2)
		ca. 450w,vbr				H_2O twist (A_2)
			465vw [b]			$\rho(SO_3)$ (A_2)
					480w	D_2O wag (B_1)
522sh,p	519sh,p	510w	508m	509w	507m	$\delta(SO_3)$ (A_1)
535w,dp	539w,dp	523sh	523m	524sh	528m	$\delta(SO_3)$ (E)
		528sh	529m			
		532w	533m	533sh		
545sh,dp		538w		538m		$\delta(SO_3)$ (E)
		543w		543sh	541m	
		547sh	546m			
			583sh		582sh	$\delta(SO_3)$ (A_2)
614w,dp	610w,dp		605sh	608sh	608s	$\delta(SO_3)$ (E)
		610vw	608s			
		616w		612vw		
		620sh	618s	621sh	617s	
			657w			H_2O wag (B_1)
			668w		666vw	
680w,p	678w,p	684w	681w	678w	676sh	$\delta(SO_3)$ (A_1)
	750m,p			739w	738s	ν(C–S) (A_1) and
				751s	749sh	ν(C–S) (E)
					753s	
762m,p		752sh				ν(C–S) (A_1)
		763s	761w			
820w,dp		827w	824m		828vw	ν(C–S) (E)
		835w	829sh			
			839m		843vw	
	945w,dp			950w	948vw	δ(DCS) (E)
				961w	962vw	
(1 027s)	(1 043s)	1 027w	1 026s	1 039w	1 044s	ν(S–O) (E)
1 030w,dp?	1 045w,dp?	1 040w	1 039s	1 048sh	1 051sh	
1 092s,p	1 092s,p	1 096vs	1 094w	1 096vs	1 098w	ν(S–O) (A_1)
1 155w,dp		1 164w	1 161w			δ(HCS) (E)
		1 181w	1 180w			
				1 182vw,br	1 179m	δ(DOD) (A_1)
1 202sh,dp		1 206w	1 197sh	1 210sh	1 192sh	ν(S–O) (E)
		1 228sh	1 204m	1 220w	1 204sh	
		1 235w	1 222s	1 230sh	1 222s	
1 240w,p?	*c*	1 250w	1 238s	1 237w	1 235s	ν(S–O) (A_1)
(1 250s,br)		1 257w	1 263s	1 246sh	1 251s	
				1 248w	1 260s	
1 258sh,dp		1 270w	1 273m	1 268w	1 272sh	ν(S–O) (E)
		1 280vw	1 249sh	1 285vw	1 294sh	
					1 442sh	δ(HOD) (A')
					1 447vw	δ(HOD) (A')
		1 644vw,br	1 639w		1 642vw	δ(HOH) (A_1)
	2 210sh,p			2 189sh		ν(C–D) (A_1)
				2 199m	2 199w	
					2 280vw	1 044 + 1 235 (=2 279)
			2 280vw			1 039 + 1 238 (=2 277)

TABLE 6 (*Continued*)

0.1mol dm^{-3} $[CH(SO_3)_3]^{3-}$ Raman (and i.r.)	0.1mol dm^{-3} $[CD(SO_3)_3]^{3-}$ Raman (and i.r.)	$K_3[CH(SO_3)_3]\cdot H_2O$ (77 K) Raman	I.r.	$K_3[CD(SO_3)_3]\cdot D_2O$ (77 K) Raman	I.r.	Assignment
				2 567w	2 569m	ν(O–D)(D_2O) (A_1)
					2 590vw	ν(O–D)(HDO) (A')
					2 627sh	ν(O–D)(HDO) (A')
				2 660w,br	2 651m	ν(O–D)(D_2O) (B_2)
2 952,mp		2 935sh				ν(C–H) (A_1)
		2 942s	2 941w		2 948vw	
		3 492w	3 490m		3 499m	ν(O–H)(H_2O (A_1)
			3 520vw		3 503sh[d]	
		3 565w	3 563m		3 570w	ν(O–H)(H_2O) (B_2)

[a] Interference from D_2O rock (B_2). [b] Observed only in the ambient-temperature spectrum. [c] Region masked by δ(DOD) of solvent. [d] Contains contribution from ν(O–H)(HDO) (A').

ature spectrum. The corresponding feature in the $K_3[CD(SO_3)_3]\cdot D_2O$ spectrum is not observed. However, a band of similar intensity is observed in the i.r. spectrum of the anhydrous salt, $K_3[CH(SO_3)_3]$, at 461 cm^{-1}, thus precluding its assignment to a water librational mode.

Having accounted for the SO_3 bending and rocking modes, bands in the 200—220 cm^{-1} region and at 170 cm^{-1} in the spectrum of the solid are assigned to the antisymmetric (E) and symmetric (A_1) CS_3 bending modes, respectively. The latter, which has a counterpart in the $K_3[CH(SO_3)_3]$ spectrum, shifts by 5 cm^{-1} on deuteriation. No assignment is made for the SO_3 torsional modes, which are expected to occur at very low frequency (<50 cm^{-1}).

Bands corresponding to the internal modes of H_2O are assigned on the basis of their isotopic frequency shifts and by their absence from the spectra of the anhydrous compound. Correlation field splitting of one O–H stretch, presumably the A_1 mode, is apparent in the i.r. spectrum. The frequencies of the O–H stretches and HOH deformation suggest that the water molecule is involved in hydrogen bonding. The minimum distance between water-oxygen atoms in the lattice (5.1 Å) precludes their involvement in hydrogen bonding with each other. Therefore, hydrogen bonding must be of the type $O(SO_3) \cdots H\text{–}O(H_2O)$.

For $K_3[CD(SO_3)_3]\cdot D_2O$ however, the assignment of i.r. bands in the O–D stretching region is based also on a study of the changes which occur in this region for samples having varying degrees of deuteriation. Due to incomplete deuteriation of $K_3[CD(SO_3)_3]\cdot D_2O$, this region also contains contributions from the HDO species. This study provides further evidence that the water molecule is involved in hydrogen bonding. The conclusion is supported by the accompanying changes in the HOD deformation region.

The i.r. spectra of partially deuteriated samples of $K_3[CH(SO_3)_3]\cdot H_2O$ at 77 K in the O–D stretching and HOD deformation regions are shown in Figure 4. In the spectrum of the least deuteriated sample (a) there are two bands in both the O–D stretching (2 622 and 2 590 cm^{-1}) and HOD deformation (1 449 and 1 445 cm^{-1}) regions. The D_2O concentration (0.1 mol %) in this sample is negligible and hence the former are also ascribed to the HDO species. Furthermore, the HDO concentration (7.7 mole %) is low enough to prevent significant correlation coupling from occurring, and hence the presence of two bands in each region is indicative of two types of HDO molecules in the crystal. This is consistent with the space group requirement that the hydrogen atoms of the water molecule are non-equivalent.

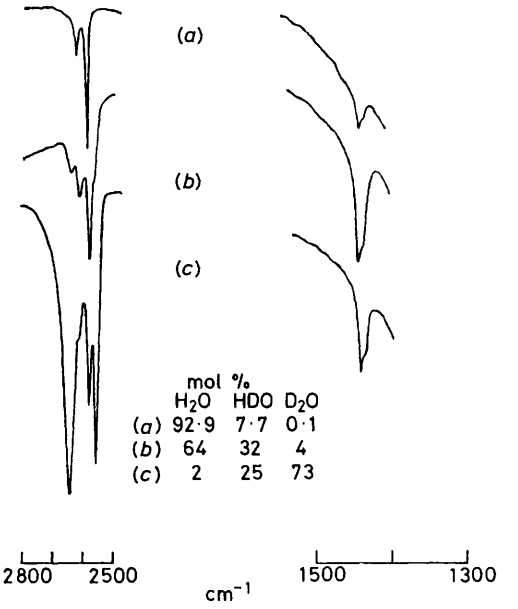

FIGURE 4 I.r. spectra of partially deuteriated $K_3[CH(SO_3)_3]\cdot H_2O$ in the O–D stretching and HOD deformation regions

On increased deuteriation [(b) and (c)], the growth of two new bands is observed in the O–D stretching region. These bands increase in intensity relative to those of HDO and are therefore assigned to the A_1 (2 569 cm^{-1}) and B_2 (2 651 cm^{-1}) modes of D_2O. Spectrum (c) represents the highest deuteriation achieved. No correlation field splitting of the D_2O modes is apparent, possibly because of masking by HDO bands. In the HOD deformation region there is no apparent change at higher deuteriations and hence the bands at 1 442 and 1 447 cm^{-1} in spectrum (c) are assigned to the deformations (A') of non-equivalent molecules.

In the region below 200 cm^{-1}, at least 14 lattice vibrations are observed. Above 200 cm^{-1}, i.r. bands ascribable to the H_2O wagging (B_1) (657 and 668 cm^{-1}) and rocking (B_2) (380 cm^{-1}) modes appear. The rocking mode is also observed in the Raman spectrum. The isotopic frequency ratio of the 380 cm^{-1} band is uncer-

tain, due to overlapping of the D_2O band by bands assigned to the SO_3 rocking modes. However, it is estimated to be *ca.* 1.36 on the basis of the intensity changes which occur in the SO_3 rocking region at about 280 cm^{-1} on deuteriation, thus precluding its assignment to a translatory mode. The wagging mode, which splits into two components under the influence of the correlation field, has an isotopic frequency ratio of 1.38. No correlation field splitting of the D_2O wag is apparent. The assignment of the band at *ca.* 325 cm^{-1} in the i.r. spectrum of the deuteriated compound to the HDO rock (A') is based on the expectation that the frequency of oscillation of the HDO molecule within the molecular (HDO) plane will be approximately mid-way between that of H_2O (380 cm^{-1}) and D_2O (estimated *ca.* 280 cm^{-1}).

The assignment of the weak Raman band at *ca.* 450 cm^{-1} to the H_2O twisting mode (A_2) is supported by its absence from the i.r. spectrum since it gains i.r. activity through solid-state effects only. The D_2O twist is not observed, probably because of masking by the relatively intense bands ascribed to SO_3 rocking modes. All bands assigned to the rotatory modes of water are absent from the spectrum of the anhydrous compound.

The isotope (D) effect on the vibrational frequencies of $[CH(SO_3)_3]^{3-}$ is in accordance with the predictions of the Teller–Redlich product rule. The observed (and calculated) products of the isotopic frequency ratios $\{[CD(SO_3)_3]^{3-}/[CH(SO_3)_3]^{3-}\}$ for the A_1 and E species are 0.714 (0.709) and 0.735 (0.709) respectively. The agreement between observed and calculated values is considered satisfactory in view of the approximations made in the calculations * and the use of fundamental rather than zero-order frequencies.

* The calculated products were determined by the method of Herzberg [17] for an XYZ_3 molecule of C_{3v} symmetry. Each SO_3 group was regarded as a single entity (Z) of 80 atomic mass units with its centre of mass at the point of half-height (0.2 Å) of the SO_3 pyramid. All CSO angles were assumed to be equal and hence the C–(SO_3) distance was taken to be 2.0 Å (1.8 + 0.2 Å). The C–H distance was taken to be 1.0 Å. The S–O stretches in the 1 200—1 300 cm^{-1} region, and the SO_3 torsions, were neglected

We thank the Australian Research Grants Committee for funds to purchase the i.r. and Raman spectrometers, J. V. Tillack for collecting the *X*-ray data, and Professor B. Penfold of the University of Canterbury, Christchurch, for the use of the diffractometer; R. A. J. acknowledges the award of a Commonwealth Postgraduate Research Scholarship, and G. S. thanks the Queensland Institute of Technology for leave to carry out the project.

[8/1750 *Received*, 9*th October*, 1978]

REFERENCES

[1] R. J. Capwell, K. H. Rhee, and K. S. Seshadri, *Spectrochim. Acta*, 1968, **A24**, 955.
[2] M. G. Miles, G. Doyle, R. P. Cooney, and R. S. Tobias, *Spectrochim. Acta*, 1969, **A25**, 1515.
[3] H. J. Backer, *Rec. Trav. chim.*, 1931, **49**, 1107.
[4] E. H. Bagnall, *J. Chem. Soc.*, 1899, **75**, 278.
[5] H. J. Backer and P. Terpstra, *Rec. Trav. chim.*, 1931, **50**, 1069.
[6] J. R. Hall and R. A. Johnson, *J. Mol. Structure*, 1978, **48**, 353.
[7] V. Seidl and O. Knop, *Canad. J. Chem.*, 1969, **47**, 1361.
[8] G. M. Sheldrick, 'SHELX–76; Program for Crystal Structure Determination,' University of Cambridge, 1976.
[9] P. A. Doyle and P. S. Turner, *Acta Cryst.*, 1968, **A24**, 390.
[10] D. T. Cromer and D. Liberman, *J. Chem. Phys.*, 1970, **53**, 1891.
[11] M. R. Truter, *J. Chem. Soc.*, 1962, 3393.
[12] F. Charbonnier, R. Faure, and H. Loiseleur, *Acta Cryst.*, 1977, **B33**, 1478.
[13] J. K. Brandon and I. D. Brown, *Canad. J. Chem.*, 1967, **45**, 1385.
[14] J. V. Silverton, D. T. Gibson, and S. C. Abrahams, *Acta Cryst.*, 1965, **19**, 651.
[15] D. R. McGregor and J. C. Speakman, *Acta Cryst.*, 1969, **B25**, 540.
[16] F. Charbonnier, R. Faure, and H. Loiseleur, *Acta Cryst.*, 1975, **B31**, 2693.
[17] G. Herzberg, 'Infrared and Raman Spectra of Polyatomic Molecules,' Van Nostrand, 1945, p. 234.